Colloids and Surfaces A 586 (2020) 124276

Contents lists available at ScienceDirect

Colloids and Surfaces A

journal homepage: www.elsevier.com/locate/colsurfa

Polyelectrolyte coated individual silica nanoparticles dispersed in concentrated divalent brine at elevated temperatures for subsurface energy applications

Esteban E. Ureña-Benavides[a,*], Ehsan Moaseri[b], Behzad Changalvaie[b], Yunping Fei[b], Muhammad Iqbal[b], Bonnie A. Lyon[c], Anthony A. Kmetz II[c], Kurt D. Pennell[c,d], Christopher J. Ellison[b,e], Keith P. Johnston[b,*]

[a] Department of Chemical Engineering, University of Mississippi, University, MS 38655, USA
[b] McKetta Department of Chemical Engineering, University of Texas, Austin, TX 78712, USA
[c] Department of Civil and Environmental Engineering, Tufts University, Medford, MA 02155, USA
[d] School of Engineering, Brown University, Providence, RI 02912, USA
[e] Department of Chemical Engineering and Materials Science, University of Minnesota, Minneapolis, MN 55455, USA

GRAPHICAL ABSTRACT

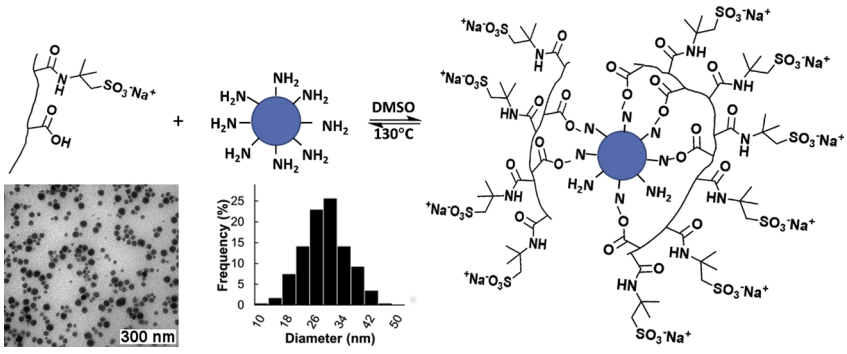

ARTICLE INFO

Keywords:
Silica nanoparticles
Poly(2-acrylamido-2-methyl-1-propanesulfonic acid-co-acrylic acid)
Nanoparticle stability
Enhanced oil recovery
CO_2sequestration

ABSTRACT

Individual sub-60 nm polyelectrolyte coated silica nanoparticles (SiNPs) were stabilized in concentrated brine at temperatures up to 120 °C. The particles have potential applications in enhanced oil recovery, CO_2 sequestration, and underground delivery of encapsulated payloads. The polyelectrolyte copolymer was grafted to modified silica particles with a general thermal method in DMSO that is broadly applicable to many types of nanoparticles and polymers with less significant hydrolysis than in aqueous based approaches. SiNPs were first coated with amine functional groups and then with poly(2-acrylamido-2-methyl-1-propanesulfonic acid-co-acrylic acid) (poly(AMPS-co-AA)) through a thermally driven amidation of the acrylic acid units in a dimethyl sulfoxide (DMSO) rich medium. Permanent aggregation and bridging were limited by controlling reaction time for temperatures up to 130 °C. The amine coated SiNP were dispersed as individual particles and the polyelectrolyte formed small flocs in DMSO. Upon transfer of the grafted SiNP from DMSO to a fully aqueous medium the hydrodynamic diameters (D_h) ranged from 30–60 nm. The particles were colloidally stable in API brine (2 wt% $CaCl_2$ and 8 wt% NaCl) at 90 °C and pHs of 5.5–9.5 for 19 days. At 120 °C, minor aggregation to 130 nm was observed after 19 days at pH 5.5, whereas the stability decreased to 1 day at neutral pH. The particles were

* Corresponding authors.
E-mail addresses: eurenab@olemiss.edu (E.E. Ureña-Benavides), kpj@che.utexas.edu (K.P. Johnston).

https://doi.org/10.1016/j.colsurfa.2019.124276
Received 16 September 2019; Received in revised form 23 November 2019; Accepted 24 November 2019
Available online 25 November 2019
0927-7757/

highly mobile in a column packed with 40–50 mesh Ottawa sand with a recovery of 82.2 % of the injected NPs. The exceptional colloidal stability and low retention in packed columns can be attributed to the steric protection of 2-acrylamido-2- methyl-1-propanesulfonic acid (AMPS) segments from particle-particle and particle-sand attractive forces, and multipoint grafting through the AA anchor groups.

1. Introduction

The role of nanotechnology continues to grow in subsurface applications including electromagnetic imaging, enhanced oil recovery, and delivery of encapsulated payloads [1–15]. Silica nanoparticles (SiNP) are inexpensive and easy to functionalize and have been used to stabilize CO_2 foams in enhanced oil recovery and CO_2 sequestration [16–24]. In subsurface reservoirs, the harsh environment of high salinity and temperatures on the order of 90 °C–150 °C presents a great challenge for colloidal stabilization of nanoparticles (NPs). In widely utilized American Petroleum Institute (API) brine, the concentrations of NaCl and $CaCl_2$ are 8 and 2 wt%, respectively. In order to achieve low retention and high mobility of NPs through porous minerals, polymeric stabilizers on the surface of the NPs can be used to provide electrosteric and/or steric repulsion between the NPs and mineral surfaces [7,10,11,14,25,26]. If the nanoparticles are small enough, on the order of 20 nm or less for silica, low molecular weight ether diol-based ligands provide sufficient steric repulsion to overcome the attractive van der Waals forces between particles [27].

The colloidal stability of polymer-coated NPs is often correlated to the solubility of the polymer at the same conditions [28]. Most water soluble polymers, including polyethylene glycol (PEG) and polyacrylamide (PAM), are not solvated well enough to be soluble at high temperature and high salinity [2,29]. Although polyacrylic acid (PAA) is soluble in concentrated NaCl at high temperature, PAA interacts strongly with Ca^{2+} resulting in salt bridging and precipitation [4,30,31]. For polyelectrolytes with strongly acidic sulfonic acid groups, the much weaker interactions with Ca^{2+} result in strong solvation in brine containing divalent cations. Examples of polyelectrolytes soluble in brine at high temperature include sulfonated phenolic resins [32], polystyrene sulfonate (PSS) and poly(2-acrylamido-2-methylpropanesulfonate) (PAMPS) [30,33,34]. Sub-50 nm silica particles end-grafted with PAMPS are colloidally stable at concentrations up to 4.5 M $CaCl_2$ [22]. In addition, various nonionic polysaccharides including polyvinyl pyrrolidone (PVP), Guar Gum and hydroxyethyl cellulose (HEC) are soluble in brine at high temperatures and have been demonstrated to improve the mobility of nanoparticles through porous media at high salinity [2,35]. Zwitterionic polymers have also been shown to stabilize graphene oxide nanoplatelets in Arab-D and API brines at temperatures up to 90 °C for over 140 days [36].

Although various methods have been explored to graft polymers to or from silica surfaces, it has been challenging to prevent formation of small aggregates during grafting. The aggregates may be produced by bridging of polymer between multiple particles or from loss of colloidal stability due to changes in surface charge upon grafting. “Grafting to” methods typically require introduction of an organic reactive group onto the silica NP surface by a condensation reaction with an alkoxysilane, or introduction of the alkoxysilane directly into the polymer [37,38]. Si-O-C bonds formed by direct condensation of organic alkoxides onto silica surfaces can undergo hydrolysis in aqueous media. “Grafting from” methods utilize surface initiated controlled polymerizations including atom transfer polymerization (ATRP) [39,40] and reversible addition-fragmentation chain transfer polymerization (RAFT) [41]. These methods provide greater control of the MW with low polydispersity, but require pre-grafting of the initiator to the NP surface. The initiators and catalysts are likely to be too expensive for subsurface applications where large quantities are utilized. Furthermore, nearly all polymers reported to date for the “grafting from” approach are not solvated at high salinity and at high temperature.

Superparamagnetic magnetite NP clusters with adsorbed [6] or grafted [7,42,43] random copolymer poly(2-acrylamido-3-methylpropanesulfonate-*co*-acrylic acid) (poly(AMPS-co-AA)) have been demonstrated to be colloidally stable in API brine up to 90 °C and 120 °C, respectively. The polymer chains, with molecular weights on the order of 200 kDa, on 100 nm particles provide steric and electrosteric repulsion and remain partially charged despite the high salinity as shown by the zeta potential (ζ) [6–8,12]. Multipoint covalent grafting of poly(AMPS-*co*-AA) has been achieved via amidation of AA units with amine functionalized IO nanoclusters using N-(3-dimethylaminopropyl)-N’-ethylcarbodiimide (EDC) catalyst [7,9,12,43]. The ~100 nm polyelectrolyte coated IO nanoclusters remain stable in API brine for 30 days at 120 °C and exhibited very low adsorption on model silica and mineral surfaces [7,43]. The low adsorption enabled high mobility through Ottawa sand, crushed Berea sandstone and consolidated Berea sandstone [7,12,43]. Covalent grafting of poly (AMPS-co-AA) to IO NP has also achieved through uncatalyzed thermal grafting in aqueous media [42]. A high concentration of amine coated IO (1 − 2 wt%) was utilized to drive the reaction, which caused some cluster growth during the grafting reaction. The uncatalyzed grafting produced stabilized IO NP in API brine at 90 °C with ultralow adsorption and outstanding mobility in crushed Berea sandstone and Ottawa sand [42]. However, the final particle size was on the order of 150 nm indicating aggregation relative to the initial 30 nm silica coated IO NPs. It was difficult to assess how much of this effect was due to changes in the NPs cores, given that the IO primary particles are weakly bound together, as well as aggregation of the nanoclusters during grafting. The aggregation may be caused by the change in ζ from positive for the amino functionalized particles (28 mV) to negative for the polymer grafted particles (-47 mV). In a fundamental study of the conformation of EDC catalyzed end-grafted carboxy terminated PAMPS homopolymer, colloidal stability of individual particles was achieved for one week in API brine at 90 °C [22]. However, this synthesis requires an extremely high polymer to NP ratio of 500:1 and the single point covalent bond may have limited stability with variations in pH.

Herein we present a new approach to synthesize individual 30–60 nm silica NPs grafted with the random copolymer poly(AMPS-co-AA) that are colloidally stable in API brine at 90 °C and 120 °C. The uncatalyzed thermal multipoint grafting of the AA groups onto aminopropyl modified silica was performed in the polar aprotic solvent dimethyl sulfoxide (DMSO, dielectric constant = 46.7) to reduce hydrolysis. The slow addition of dilute aminopropyl functionalized silica at 0.25 wt% into a solution of poly (AMPS-co-AA), and limited reaction time, mitigated permanent bridging of the polymer chains to more than one particle. The reaction time was optimized to be sufficiently long for grafting, but short enough to minimize bridging. The presence of grafting was characterized by TGA, ζ and by the stability of the grafted NPs in API brine at 90 °C and 120 °C. The particle size distribution was determined by dynamic light scattering (DLS) in deionized water and API brine and by transmission electron microscopy (TEM). Individual NPs were stable for 19 days without detectable aggregation at 90 °C at pH 5.5 and 7.5; at pH 9.5 only minor growth was observed. Moreover the individual NP were stable in API brine at 120 °C for 1 day at pH 5.5 and 7.5. Mobility tests in a column packed with 40–50 mesh Ottawa sand showed 82.2% recovery of the SiNP dispersed in API brine. The SiNP designed herein have potential applications in in enhanced oil recovery, CO_2 sequestration and underground payload delivery.

Table 1
Hydrodynamic diameters (D_h) from volume distribution with cumulative %V in parenthesis and zeta potential (ζ) of pure poly(AMPS-co-AA) in DI water and API brine at pH 7 and in DMSO.

Conditions	D_h, nm (Cumulative, %V)
DI water at 25 °C	7(54) - 23(96)
DI water at 90 °C	7(69) - 24(95)
API brine at 25 °C	13(57) - 18(94)
API brine at 90 °C	7(56) - 24(94)
90% DMSO at 25 °C	592(64) - 717(97)
90% DMSO at 80 °C	150(76) - 305(99)

2. Experimental Section

2.1. Materials

Silica nanoparticles were purchased from Nyacol Nanotechnologies (Ashland, MA), 3-amniopropyl triethoxy silane (APTES), dimethyl sulfoxide, acrylic acid (AA), potassium persulfate, and sodium metabisulfite were acquired from Sigma-Aldrich (St. Louis, MO) and Fisher Scientific (Pittsburgh, PA) and used as received. The monomer 2-amino-2-methylpropanesulfonate (AMPS) was a gift from Lubrizol corporation and used as received.

2.2. Synthesis of poly($AMPS_3$-co-AA_1)

The copolymer synthesis with an AMPS/AA ratio of 3 was done following our previously reported procedure [7,12]. A three-necked round bottom flask was loaded under nitrogen with 30.9 g (0.135 mol) of AMPS, 4.86 g (0.018 mol) of potassium persulfate and 3.42 g (0.018 mol) of sodium metabisulfite; then 180 mL of degassed water and 3.0 mL (0.044 mol) of AA were added. The reaction was stirred for 16 h at 80 °C, after which the final ratio of monomers was determined by 1H NMR. The molecular weight was estimated based on the hydrodynamic diameter according to a previously published correlation [7,8]. The degree of polymerization was approximately 1000 while the MW was 200 kDa.

2.3. Amine coating

Coating of aminopropyl groups on the silica surface was based on our earlier methods [12,42]. Briefly, 160 mL of 5 wt% acetic was added to a media bottle, followed by addition of 16 mL of APTES. APTES oligomerization was allowed to occur for 20 min after which the pH was brought up to 8 with 70 mL of 1 N NaOH. Silica NP were added dropwise while stirring the mixture; at this point the mixture turns cloudy. The reaction mixture was heated to 65 °C, and allowed to stir for 20 h; the final suspension turns light blue and clear at the end of the reaction. Purification was done by diafiltration using 30 kDa centrifugal filters (Amicon Ultra – 15) from EMD Millipore (Billerica, MA). To each tube, 15 mL of mixture were added and centrifuged at 5500 rpm until the retained volume was 2 mL; 10 mL of DI water were added, followed by centrifugation. A total of 4 cycles of water addition and centrifugation were done. The final suspension was concentrated to 50 mg/mL, then 16 mL of APTES coated NP were added dropwise to 144 mL of DMSO to get a final silica concentration of 5 mg/mL in 90 % DMSO/10 % water.

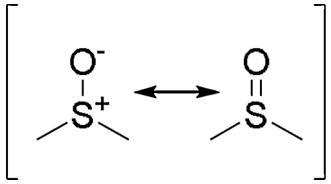

Scheme 1. Resonance structures of DMSO.

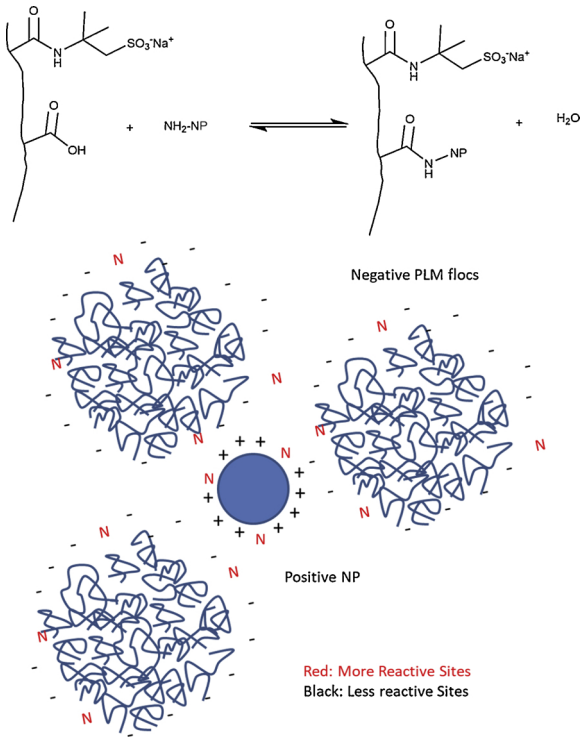

Fig. 1. Schematic of uncatalyzed heat driven grafting in DMSO. N refers to neutral charge, i.e. protonated carboxylate or unprotonated amine.

2.4. Poly(AMPS-co-AA) grafting

Silica NP were grafted in a DMSO/water mixture. DMSO (3.2 mL) was added to 1.45 mL of an aqueous copolymer solution at pH 5 with an initial concentration of 15 wt %. The silica NP dispersion (4.35 mL) was mixed with the polymer dispersion to produce a final concentration of 0.24 wt % silica and 2.4 wt% polymer, and a solvent composition of 80% DMSO/20% water. The mixture was then heated in an open flask to the desired reaction temperature (90 °C or 130 °C) while stirring. Quenching of the reaction was achieved by cooling the mixture and diluting the product 3-fold in DI water at room temperature. The DMSO was removed first by diafiltration with 30 kDa pore size regenerated

Table 2
Summary of colloidal and surface properties of amine coated and naked silica nanoparticles.

Property	Naked SiNP	APTES coated SiNP
D_h in DI Water, nm (Cumulative, %V)	20(48) – 22(81) – 49(98)	36(52) – 44(81) – 59(98)
D_h in DMSO, nm (Cumulative, %V)	—	26(56) – 29(82) – 33(98)
ζ at pH 5, mV	−27.8 ± 5.3	29.4 ± 2.5
ζ in 90% DMSO, mV	—	36.5 ± 1.8
Amine content, μmol/mg	—	3.5 ± 0.9
TGA wt. loss, %	2.1 ± 0.2	5.4 ± 0.8

cellulose centrifugal filters (Amicon Ultra – 15), then completing two cycles of 15 mL DI water addition followed by concentration to 2 mL. Excess polymer was then removed by diafiltration, concentrating the grafted SiNP to 2 mL in 300 kDa pore size PES centrifugal filters (Vivaspin 20) from Sartorius (Bohemia, NY).

2.5. Amine titration

The amine content was measured following an earlier report [44]. Amine coated silica NP were diluted in DI water (200 μL sample in 50 mL water). The pH was then adjusted to 9.3 with 1 N NaOH. The resulting mixture was then titrated with 0.01 N HCl, while measuring conductivity and pH, until the pH was less than 5.

2.6. Dynamic light scattering (DLS) and ζ measurements

The hydrodynamic diameters (D_h) were measured using dynamic light scattering (DLS) with a Brookhaven ZetaPlus system from Brookhaven Instruments Co. (Holtsville, NY) at a measurement angle of 90° [12]. The NNLS algorithm was used to fit the autocorrelation functions. Measurements were collected over 1 min with a count rate of at least 300 kcps, except for long term stability data, which was obtained at a count rate of at least 30 kcps. That is because the concentration of those samples was 0.5 mg/ml. Two measurements were done per sample and care was taken to ensure the autocorrelation function could be properly fit. Zeta potential measurements were made following our previous publication [12].

2.7. High temperature high salt (HTHS) stability test

A 0.500 mL sample of poly(AMPS-co-AA) coated NPs was taken and diluted in 1.000 mL of API brine, then 0.500 mL of 200% API brine was added to maintain a salt concentration equal to 100% API brine. The resulting silica concentration was 0.5 mg/mL. The pH was adjusted with NaOH and the samples were then filtered through a 450 nm syringe filter into an ACE glass (Vineland, NJ) pressure tube, previously washed with filtered API brine. The samples were heated to 90 or 120 °C for the desired amount of time, and then sampled to measure the hydrodynamic diameter with DLS.

2.8. Thermogravimetric analysis (TGA)

The organic content of the SiNPs at the various stages was determined using TGA. A Mettler-Toledo (Columbus, OH) TGA/SDTA851e instrument was run with N_2 atmosphere. The temperature was ramped from 25 to 120 °C at a heating rate of 10 °C/min and allowed to remain constant for 15 min to remove any adsorbed water; the temperature was ramped again to 900 °C at the same heating rate.

2.9. Transmission electron microscopy (TEM)

A FEI (Hillsboro, Oregon) TECNAI Spirit Bio Twin was used to obtain TEM images. A dilute dispersion of the silica NP was allowed to dry on a 400 mesh Formvar-coated copper TEM grid, then imaged in the TEM.

2.10. Mobility test of polymer grafted silica NPs

Nanoparticle mobility was tested in a column packed with approximately 95 g of 40 − 50 mesh Ottawa sand (specific surface area = 0.0125 m^2/g) as a model porous medium. The column details and procedure are described in our previous publication [12]. The packed column had column porosities near 0.37. It was initially purged with CO_2 for 20 min, and then subjected to an injection of 10 pore volumes (PV) of API brine solution. The poly(AMPS-co-AA) grafted SiNPs were then injected at neutral pH with a concentration of 250 mg/L at a flow rate of 1.8 mL/min, equivalent to a pore-water velocity of 2.9 m/day. A total 4 PV of NPs dispersion were added, which was followed by an equal flow rate of 3 PV of API brine background solution. Samples were collected from the effluent to measure silica concentration using a Varian 710 Inductively Coupled Plasma-Optical Emission Spectrometers (ICP-OES) from Agilent (Santa Clara, CA). The SiNPs were

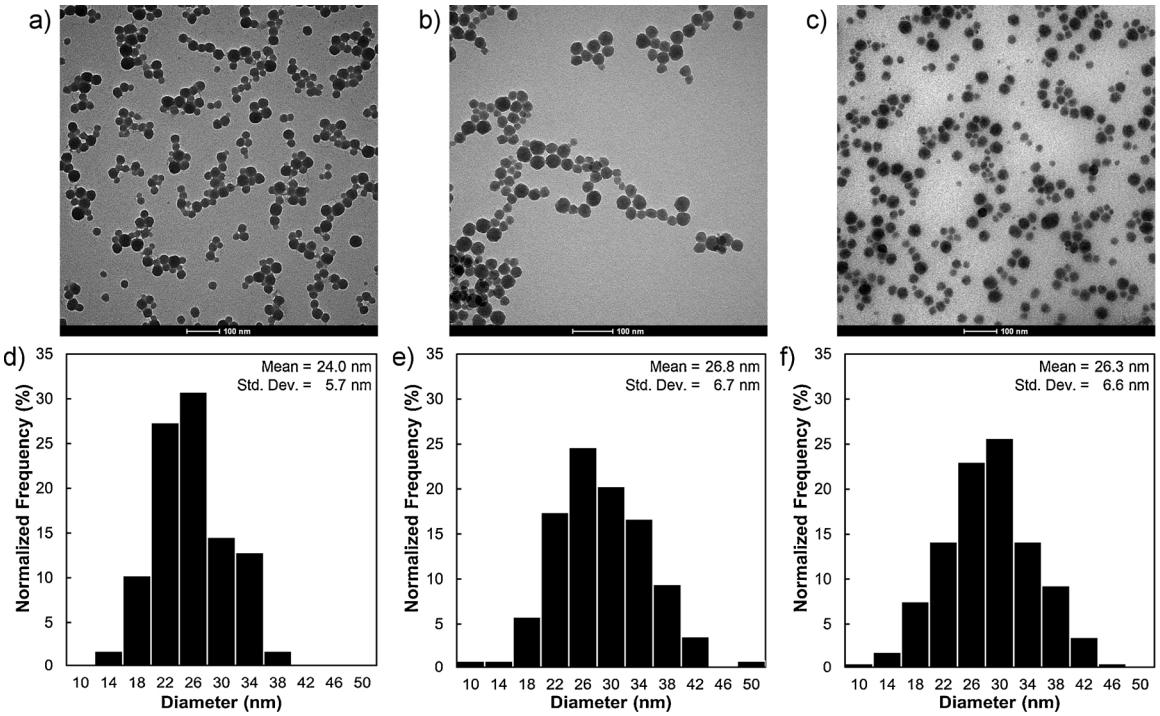

Fig. 2. TEM images of a) initial, b) amine coated, and c) poly($AMPS_3$-co-AA_1) coated SiNP cores. Size distributions of d) initial, e) amine coated, and f) poly($AMPS_3$-co-AA_1) coated SiNP cores.

digested in 2.5 N NaOH for 24 h and then diluted with DI water up to 0.5 N NaOH. The calibration curve was prepared using TraceCert Silicon Standard (1000 mg/l).

3. Results and discussion

3.1. Colloidal properties of starting materials

Poly(AMPS-*co*-AA) functionalized silica nanoparticles were prepared by thermal amidation in DMSO rich medium and the thermal stability was established in API brine at 90 °C and 120 °C for 19 days. In order for a grafted polymer to sterically stabilize a NP in a specific medium the polymer itself must be solvated and soluble [28]. Hydrodynamic diameters (D_h) of poly(AMPS-*co*-AA) in water, API brine and DMSO are shown in Table 1. The D_h values are given as points of a volume distribution with their respective cumulative %V in parenthesis. The measurements in water at room temperature (RT) show 54% of the polymer volume is composed of chains that are 7 nm, or less; while 96% of the polymer volume corresponds to chains equal to, or less than, 23 nm. Heating the polymer solution to 90 °C in water, dissolving it in API brine at RT, or heating to 90 °C in API brine did not cause any significant global change in the D_h of poly(AMPS-co-AA). Therefore, the polymer is solvated sufficiently in each case to provide steric stabilization. The poly(AMPS-co-AA) used in this study was made by free radical polymerization, since the cost of controlled polymerization methods can be strongly prohibitive for underground applications like EOR and CO_2 sequestration.

The zeta potential (ζ) at pH 5.5 of the pure polymer was -41.4 ± 0.8 mV in aqueous solution; at these conditions the sulfonates are fully deprotonated and the carboxylates are partially deprotonated. When the polymer was transferred to a solvent mixture of 90% DMSO/10% water, ζ was -39.8 ± 1.5, and the D_h was 592(64) - 717(97) nm [45]. The polymer flocculated in the DMSO-rich solvent despite remaining charged. This result is consistent with literature reports that DMSO solvates anions weakly, compared to cations that are more strongly solvated [46,47]. Increasing the temperature to 80 °C indicated a lower D_h in the DMSO rich mixture, however the polyelectrolyte remained highly flocculated compared API brine and DI water.

The colloidal and surface properties of bare silica and aminopropyl functionalized silica NPs are shown in Table 2. The starting SiNPs have D_hs of 20(48) - 22(81) - 49(98) nm. [45] After amine coating the size increased only modestly to 36(52) - 44(81) - 59(98) nm [45]. Modification of the silica surface was confirmed by the change in ζ at pH 5 from -27.8 ± 5.3 mV for bare silica to 29.4 ± 2.5 mV for amine functionalized silica. From conductometric titration, the amine surface concentration was 3.6 ± 0.9 μmolNH_2/mg silica. As opposed to the anionic poly(AMPS-co-AA), the amine coated particles are highly stable in 90% DMSO, evidenced by D_hs of 26(56) - 29(82) - 33(98) nm [45], and a ζ of 36.5 ± 1.8 mV. The result is again consistent with the typical behavior of DMSO, which stabilizes cations much better than anions [46,47].

3.2. Uncatalyzed amidation

The pK_a of carboxylates vary greatly from water to DMSO; for example the pK_a is 4.8 for acetic acid in water at RT, and much higher, 12.6 in DMSO [48,49]. Thus the AA units in poly(AMPS-co-AA) are likely protonated in DMSO, while in water at pH 5, mostly deprotonated. Sulfonates are much more acidic and are expected to remain deprotonated in both water and DMSO; for example, methanesulfonic acid has a pK_a of -2 in water and -1.6 in DMSO [50]. The pK_a of cationic ammonium compounds usually does not change significantly in DMSO compared to water. For example, n-butylammonium has a pK_a of 10.61 in water and 11.1 in DMSO [51]; thus, we expect amine groups on coated particles to be mostly protonated and positively charged in DMSO. These observations are consistent with the measured ζ's of poly(AMPS-co-AA) and of amine coated SiNPs shown in Tables 1 and 2. The ability of DMSO to stabilize charged compounds, especially cations, is partly attributed to the resonance structure shown in Scheme 1; the S—O bond order is estimated to be 1.5 [46], thus approximately half of the solvent is charged with an exposed negative oxygen and a positive sulfur atom.

The uncatalyzed amidation reaction is known to proceed faster and to a greater extent when the amine and the carboxylic acid are both neutral [47,52], as is the case for the acrylic acid units on the polymer in this study. On the contrary, a large proportion of the amines on the surface of the NP will be positively charged; however, successful grafting of poly(AMPS-co-AA) onto the APTES-SiNP, indicate sufficient reactivity of the amine towards the amidation reaction. Furthermore, a high grafting temperature also helps drive the reaction to completion.

Successful coating of individual NP with poly(AMPS-co-AA) requires avoiding aggregation and bridging of the silica NP during grafting. As shown in Fig. 1, we expect the stable positively charged silica NP will approach the negative poly(AMPS-co-AA) flocs leading to grafting. During reaction the polymer chains are not fully solvated. It is reasonable to assume the amine coated silica NPs do not diffuse into the polymer flocs, in which the polymer chains have limited mobility. The system studied herein represents a relatively uncommon situation, i.e., a partially lyophobic polymer grafted onto lyophilic nanoparticles. Our results suggest that upon transferring to a good solvent individually dispersed NPs are obtained.

The reason for the efficient grafting when the polymer chains are not fully solvated is not entirely understood. The 200 kDa poly(AMPS-co-AA) used herein has a hydrodynamic diameter of 10 nm in 1 M NaCl solution when it is solvated [7]. The large polymer flocs may potentially help to keep the 30 nm NPs further apart during grafting to prevent bridging. Thus, it is possible the polymer flocculation was beneficial although experiments in a good nonaqueous solvent would be needed to prove this. Even if nonspecific bridging of two NPs by physisorbed poly(AMPS-co-AA) occurs during grafting, this bridging may dissociate upon transfer from DMSO into a the good aqueous brine solvent if they are not covalently attached,. In addition, a moderate SiNP concentration (0.24 – 0.29 % wt) and slow addition to the polyelectrolyte solution lowers aggregation by decreasing the number of collisions between NP in the presence of the large excess of polyelectrolyte.

3.3. Colloidal stability of poly(AMPS-co-AA) grafted silica nanoparticles in extreme environment

Upon grafting, the particles were transferred to water by diafiltration using centrifugal filters. In the resulting aqueous suspension, the

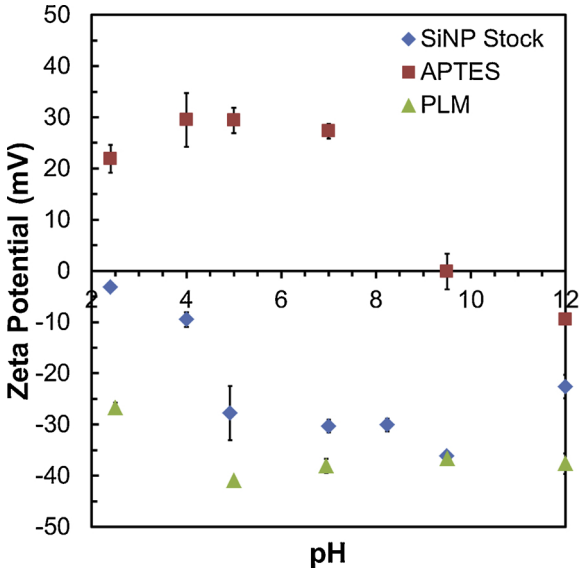

Fig. 3. Zeta Potential (ζ) of starting silica NP, APTES coated and poly(AMPS-co-AA) (PLM) coated NP; grafted at 130 °C for 12 h.

Table 3
Reaction time optimization. Hydrodynamic diameters of poly($AMPS_3$-co-AA_1) coated NP are given in DI water or API brine as a function of grafting time and reaction temperature. The ratio of poly(AMPS-co-AA) to silica NP is 10 g/gSilica with a silica concentration of 0.29 % wt. Initial amine coated SiNP D_h: 36(52) - 44(81) - 59(98).

Reaction Time (h)	Hydrodynamic diameters, nm (Cumulative % Vol)							
	90 °C Reaction				130 °C Reaction			
	DI Water	API at RT	API at 90 °C	API at 120 °C	DI Water	API at RT	API at 90 °C	API at 120 °C
0.25	44(58) 51(88) 169(93)	475(12) 1422(72)	UMC[a]	UMC[a]	35(54) 37(74) 148(94)	89(49) 336(88)	UMC[a]	UMC[a]
1	30(20) 90(53) 121(90) 328(95)	472(64) 1462(83)	UMC[a]	UMC[a]	46(47) 55(75) 148(93)	21(54) 24(89) 90(97)	Precip.	Precip.
3	85(43) 98(82) 222(94)	72(5) 453(82)	UMC[a]	UMC[a]	73(44) 85(94)	42(64) 54(87) 71(97)	Precip.	Precip.
12	67(43) 167(85) 2079(96)	27(51) 32(86) 142(97)	182(43) 6300(79)	UMC[a]	45(61) 50(86) 139(96)	38(41) 40(73) 46(97)	48(49) 57(77) 66(93)	47(49) 67(69) 195(86)
24	83(41) 89(61) 175(81)	25(49) 71(71) 122(96)	64(59) 74(81)239(93)	240(38) 5635(62)	62(56) 72(91)	43(54) 55(99)	47(33) 54(62) 73(97)	83(8) 448(47)
72	116(49) 127(66) 318(97)	28(67) 32(86) 120(98)	60(35) 63(66) 71(95)	204(30) 6383(60)	45(47) 52(79) 118(96)	43(63) 51(96)	40(30) 80(56) 137(98)	UMC[a]

[a] UMC stands for unstable at milder conditions.

poly(AMPS-co-AA) flocs break apart, releasing ungrafted chains into solution, which can be then removed as the diafiltration proceeds. The covalently attached chains, which were originally collapsed in DMSO, are expected to extend in water and provide electrosteric stabilization to the silica NP. The TEM images in Fig. 2 show the silica cores from the initial state to the final polymer coated NP. The size distributions from TEM in Figs. 2d, e and f indicate no growth or clustering of the SiNP cores throughout the two step coating process. Individual polymer grafted silica NPs were obtained in this work demonstrating that aggregation and interparticle bridging were successfully avoided, contrary to the reaction in aqueous phase where IO NP grew from 30 nm to 150 nm [42].

The ζ as a function of pH in aqueous media was measured throughout the different synthesis steps (Fig. 3). The SiNPs are negative over the whole pH range. The ζ of the amine coated particles was +30 mV at pH 5 and becomes 0 at the isoelectric point at 9.5. The highest stability region for the aminopropyl functionalized particles is between pH 4 and 7, where the ζ remains close to +30 mV. These results are consistent with ζ values measured for silica coated iron oxide, and subsequent amine functionalization [44,53]. After poly(AMPS-co-AA) grafting, the ζ decreases substantially and becomes highly negative from pH 2.5–12. At pH 2.5, the sulfonate groups are expected to remain charged, while the AA units are protonated; under these conditions the measured ζ was -27 mV. When the pH was increased to 5, the carboxylate groups deprotonated and the ζ decreased to −40 mV, then remained virtually unchanged up to pH 12 indicating a substantial level of grafting.

The colloidal stability of NPs can be perturbed while mixing the NP dispersion with the polymer depending upon changes in the surface charge, along with potential bridging of the polymer chains between particles. For the different mixing protocols shown in Table S.1, there were minimal differences in the stability of the grafted NP in DI water and in brine demonstrating the robustness of the grafting techniques. Since none of the methods provided significantly better stability than the others, the fastest and simplest was chosen; dropwise addition of amine SiNP to a polyelectrolyte solution over a period of 1 min. In most cases, the measured D_h values in DI water were larger than in brine. The only exceptions occurred when the polymer flocs were disturbed during mixing by bath sonicating, or by heating to 90 °C prior to mixing. In the former, the D_h was smaller in DI water than in brine, while in the latter they were equal. The D_h reduction in brine may be explained in part by contraction of polyelectrolyte chains as electrostatic repulsion between the charges is screened by the added electrolyte in the double layer [7,22,54]. Moreover, specific interactions of Ca^{2+} with unreacted carboxylates can cause bridging inside the polyelectrolyte shell within a given particle to further decrease the size.

The effects of reaction time and temperature were optimized by studying the colloidal stability of the polymer grafted NP at increasingly harsh conditions: brine at RT, 90 °C and 120 °C. It is ultimately desired to achieve substantial colloidal stability in brine at elevated temperature in order to use the nanoparticles in subsurface energy applications. When the NP were grafted at 90 °C for 3 h or less, significant aggregation occurred in API brine at room temperature as shown in Table 3 indicating insufficient time for grafting. These particles were not tested at higher temperatures as they failed the mildest stability test at RT. From the TGA traces shown in Fig. 4a, significant amounts of adsorbed and grafted polymer were present, yet the adsorption was presumably weak leading to aggregation in API brine at RT. When the grafting time was increased to 12, 24 and 72 h, the resulting grafted NP remained stable in API brine at RT. The NPs grafted for 12 h aggregated in API at 90 °C, whereas at 24 and 72 h reaction times the NPs were stable. However, these particles aggregated at 120 °C in API brine, suggesting the possibility of an insufficient amount of grafted polymer on the SiNP surface.

The reaction temperature was raised to 130 °C in order to further increase the level of grafting by accelerating reaction kinetics and water evaporation from DMSO. A marked stability enhancement was observed in the D_h values in Table 3 compared to the aforementioned systems grafted at 90 °C. Here, all the NP, with the exception of those

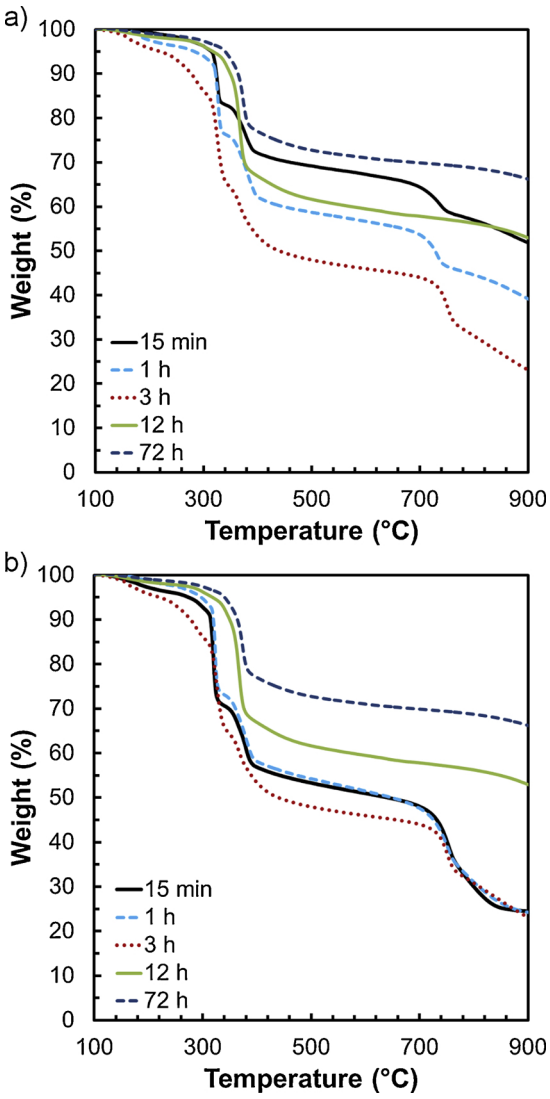

Fig. 4. TGA traces of silica coated NP at various reaction times for particles grafted at a) 90 °C and b) 130 °C.

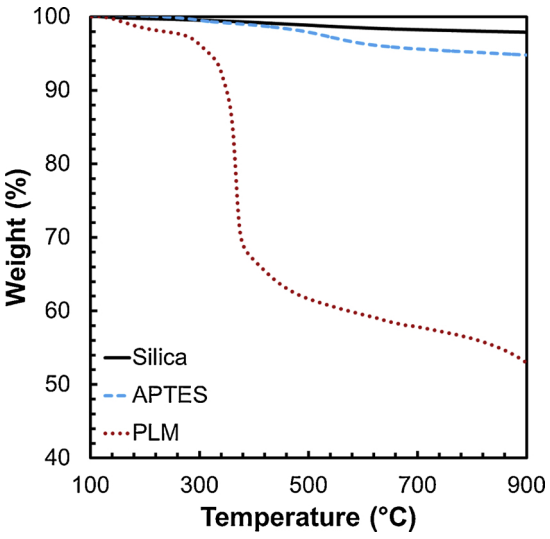

Fig. 5. TGA traces of the starting silica NP, APTES coated NP, and poly(AMPS-*co*-AA) silica NP grafted at 130 °C for 12 h.

reacted for only 15 min, remained stable in API brine at RT. At 90 °C and 120 °C in API brine, the samples grafted for 1 and 3 h precipitated. At 120 °C, particles grafted for a long time of 24 h grew to 448(47) nm. Interestingly, the particles grafted for an intermediate time of only 12 h remained stable as reflected in the small D_h values. These conditions were the best in this study for minimizing particle size in API brine at 120 °C. Furthermore, these particles underwent much less contraction from DI water to API brine at RT relative to the other samples

For grafting times up to 3 h, the TGA traces (Fig. 4b) were similar whereby 67 wt % of poly(AMPS-co-AA) was present on the NP surface either grafted or physically adsorbed. However, for the optimal grafting time of 12 h, the polymer content from TGA was smaller, 40.5 wt %, and dropped to 25.4 wt % at 72 h. These decreases may be attributed to amide bond hydrolysis leading to cleavage of grafted polymer, or a decrease in poly($AMPS_3$-co-AA_1) physisorption at longer reaction times. Fig. 4 shows the presence of maxima in polymer content with reaction time. For reaction temperatures of 90 °C and 130 °C, the maxima appear to be near 3 h, which does not match the optimum time for highest colloidal stability. This difference may reflect the influence of physisorption, present in the TGA results, versus chemical grafting that maintains polymer on the surface during long term stability tests. It is thus likely the non-monotonous behavior of copolymer content with reaction time is due to both the reversibility of the amidation reaction and a lower amount of physisorption at longer reaction times.

Fig. 5 shows the weight loss upon increasing temperature of the starting silica NP, amine coated, and polymer coated particles (grafting at 130 °C for 12 h). The silica NP only loses 1.9 wt% between 100 and 850 °C, which may come from dehydration of the surface silanols (Si-OH). The amine coated particles lose a total of 5.1 wt % within the same temperature range, mostly from aminopropyl cleavage and Si-OH. The polymer coated particles have a total weight loss of 45.1 % wt which includes the polymer, aminopropyl and Si-OH dehydration. Thus results the final NPs contain 54.9 wt % silica, 3.0 wt % aminopropyl and 42.1 wt % poly($AMPS_3$-co-AA_1).

The thickness of a collapsed polymer shell can be estimated from the average TEM diameter of the amine functionalized NP and TGA composition. If the density of a collapsed polyelectrolyte shell is 1 g/mL (density of the bulk polymer) then the thickness would be 5.4 nm, and the respective NP diameter 37.7 nm according to TEM. The measured D_h of the pure polyelectrolyte ranged from 7 to 13 nm (Cumulative ~ 55 %V), and for the polymer coated NP varied from 30 to 50 nm (Cumulative ~ 50 %V). Considering the polymer shell should remain hydrated in API brine, and a starting D_h of 27 nm for the APTES coated particles, the DLS, TEM and TGA measurements suggest approximately one monolayer of polymer was coated on individual nanoparticles.

An extreme dilution test was done for the NP grafted at 90 °C during 24 and 72 h, as well as NP grafted at 130 °C for 12 and 24 h. The nanoparticles were diluted 100-fold and washed twice to remove any physically adsorbed polymer. All four samples remained stable with negligible changes in D_h in API brine after this dilution test, indicating the polymer was covalently attached and not just physically adsorbed. As a control for the extreme dilution test, samples with adsorbed (rather them chemically grafted) polymer were prepared by mixing the amine coated NP with poly(AMPS-co-AA) at RT in DI water and in DMSO. The mixtures were stirred for 16 h to allow adsorption. After purification and extreme dilution, the D_h in brine were in the order of 1 μm, which would be consistent with aggregation after desorption of the non-covalently grafted polymer.

The long-term stability of the polymer coated nanoparticles in API brine was studied versus pH at 90 °C and 120 °C as shown in Table 4. At 90 °C, the small change in D_hs indicated outstanding stability for all three pH values after 19 days. Even at the extremely harsh temperature of 120 °C, the NP did not aggregate at pH 5.5 and 7.5 after aging for 1 day, but did aggregate at pH 9.5 which may result from alkaline hydrolysis of the amide bonds, thus reducing the stability. For longer aging times the NP at pH 7.5 aggregated and sedimented. In contrast,

Table 4
Hydrodynamic diameters (Cumulative, %V in parenthesis) of poly($AMPS_3$-co-AA_1) coated SiNP (0.5 mgSilica/mL) as a function of aging time in API brine at 90 °C and 120 °C. Grafted at 130 °C for 12 h.

pH	Aging Time (days)	API brine at 90 °C	API brine at 120 °C
5.5	0 (RT)	48(54) – 64(95)	52(42) – 62(92)
	1	50(58) – 60(96)	63(47) – 73(71) – 101(92)
	4	37(46) – 56(94)	140(45) – 230(94)
	11	50(50) – 60(95)	330(64) – 560(96)
	19	63(59) – 88(97)	133(73) – 178(97)
7.5	0 (RT)	42(61) – 71(97)	51(40) – 65(90)
	1	31(55) – 34(88) – 75(95)	46(60) – 54(74) – 256(90)
	4	62(45) – 74(92)	Precipitated
	11	34(67) – 37(88) – 89(97)	
	19	26(53) – 31(88) – 81(96)	
9.5	0 (RT)	32(48) – 42(74) – 72(97)	24(64) – 27(93)
	1	28(52) – 33(84) – 78(93)	113(10) – 477(66) – 815(96)
	4	40(49) – 47(84) – 124(96)	Precipitated
	11	79(47) – 97(75) – 119 (91)	
	19	62(55) – 78(97)	

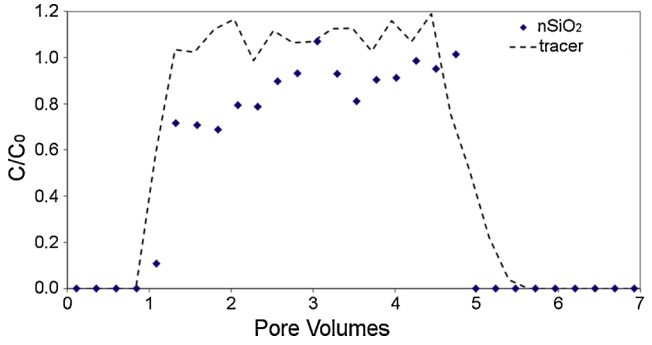

Fig. 6. Mobility of polymer grafted SiNPs (130 °C for 12 h) in API brine saturated column packed with 40–50 mesh Ottawa sand. The input concentration was 250 mg/L at room temperature and pH 7 resulting in a breakthrough of 82.2% and 3.1 mg/m^2 retention.

the NP at pH 5.5 grew but then remained stable after 19 days with D_hs of 133(73) - 178(97) nm.[2] There appears to be a drop in size from 11 days to 19 days. The reasons for this behavior are uncertain, however it could be due to a selective sedimentation of larger aggregates leaving smaller ones dispersed in brine.

The stability of the silica nanoparticles may be due to electrosteric stabilization and efficient multi-point grafting of poly(AMPS-co-AA) onto their surfaces. With multiple attachment points the chains will remain grafted even after hydrolysis of one (or even a few) graft point (s). Moreover, the uncatalyzed heat driven amidation in DMSO was found to be sufficient for grafting of polymer aggregates to the nanoparticle surfaces. It is unknown whether the presence of the polymer aggregates prior to grafting increased or decreased the graft density. In most cases shown in Table 3, the D_h was larger in DI water than in API brine. The contraction of the polyelectrolyte shell in brine may be attributed to charge screening with the large salt concentration. Another possibility is that the Ca^{2+} ions in API brine produced bridging of polymer chains on each particle that cause greater contraction than would be expected simply from Debye screening in the double layer. This contraction could even cause break up of aggregates of silica nanoparticles by reducing the amount of interparticle polymer bridging. In API brine, electrostatic stabilization is much weaker than in DI water; however, the polymer continues to provide steric stabilization as long as it remains hydrated and attached to the NP surface. The AMPS units, which have negligible affinity for divalent ions like Ca^{2+}, are highly solvated in the extreme harsh environment studied here. The number of multipoint attachment sites for the polymer coating is highly relevant, as it will influence how far out the polymer chains extend from the surface. As the degree of chain extension increases the steric stabilization increases, but so does the potential for interparticle bridging. An accurate quantification of the number of attachment sites per polymer chain remain extremely challenging. To our knowledge this is the first time a suspension of individual polymer grafted nanoparticles smaller than 60 nm have been stabilized in API brine at temperatures up to 120 °C, with long term stability at 90 °C for 19 days. However, Ranka et al. recently stabilized 60 nm silica NP for 30 days in Arab D brine (up to 120 000 mg/dm^3) at 90 °C [55].

3.4. Mobility of poly(AMPS-co-AA) grafted silica nanoparticles

To study the mobility and stability of the polymer grafted silica NPs, the transport of the NPs was investigated in a column packed with 40–50 mesh Ottawa sand as a model porous medium. Fig. 6 presents the effluent breakthrough for polymer grafted silica NPs (polymer grafting at 130 °C for 48 h) in API brine saturated 40–50 mesh Ottawa sand column. A pulse of NPs (250 mg/L) were injected to the column, continued by injection of API brine until the concentration of silica NPs became undetectable. The initial breakthrough was observed at 1 PV, followed by significant increase in concentration of NPs in the effluent (i.e. $C/C_0 = 1.0$). After almost 4 PV, the effluent concentration drops sharply down to undetectable values, which corresponds to the injected pure API brine. The recovered silica NPs in the effluent was ~82.2 % of the injected NPs, corresponding to a retention under dynamic conditions of 3.1 mg/m^2. Such a low retention value can be attributed to weak interactions of the polymer chains grafted on the silica NPs with the surfaces of the sand particles in the packed bed. The AMPS chains provide stability of the silica NPs by sterically hindering NP-substrate interactions and overcoming the van der Waals attraction forces between them.

4. Conclusions

Individual silica NPs were grafted with poly(AMPS-*co*-AA) in the colloidal state using a multi-point “grafting to” technique, whereby the nanoparticles did not undergo bridging, aggregation or core growth. The polymer coated silica nanoparticles with hydrodynamic diameters ranging from 30–60 nm were stable in API brine at 90 °C for 19 days without any detectable aggregation at pH 5.5 and 7.5, while at pH 9.5 the hydrodynamic diameter remained between 60 and 90 nm. Moreover, in the extremely harsh environment of API brine at 120 °C the silica NPs remained stable after 1 day at pH 5.5 and 7.5. The polymer was grafted by a novel thermal amidation of AA units onto amine functionalized silica NPs in DMSO without the need for a

catalyst. An advantage of DMSO versus water as the solvent is the diminished amide hydrolysis as well as the higher boiling point. Upon two consecutive dilutions by a factor of 100 each, the NPs remained stable in brine indicating the covalent grafting of poly(AMPS-*co*-AA) onto the NP surface was permanent. The highest colloidal stability was achieved when the grafting reaction was performed at 130 °C for 12 h. Longer reaction times may lead to bridging or amide bond hydrolysis reducing the amount of grafted copolymer, while reaction times of 3 h or less resulted in insufficient grafting for colloidal stability of the nanoparticles in brine at high temperature. The amine coated SiNPs, pure poly(AMPS-*co*-AA), and polyelectrolyte coated nanoparticles were all charged in DMSO, as indicated by ζ potentials of 36.5 ± 1.3, -39.8 ± 1.5 and -33.0 ± 4.7 mV respectively. After the amidation reaction, the particles were easily transferred to water by diafiltration and remained unaggregated throughout the purification process. To the knowledge of the authors this is the first report of individual polymer grafted nanoparticles smaller than 60 nm stable in concentrated brine at 120 °C with long term stability at 90 °C. These harsh conditions mimic those encountered in underground applications like enhanced oil recovery, CO_2 sequestration and payload delivery.

Author contributions

Esteban E. Ureña-Benavides: Conceived and designed the analysis, Collected the data, Performed the analysis, Wrote the paper, Other contribution

Ehsan Moaseri: Collected the data

Behzad Changalvaie: Collected the data

Yunping Fei: Collected the data

Muhammad Iqbal: Collected the data

Bonnie A. Lyon: Collected the data

Anthony A. Kmetz II: Collected the data

Kurt D. Pennell: Contributed data or analysis tools, Other contribution

Christopher J. Ellison: Contributed data or analysis tools, Other contribution

Keith P. Johnston: Conceived and designed the analysis, Other contribution

Declaration of Competing Interest

None.

Acknowledgements

This work was supported by the Advanced Energy Consortium (Member companies include Total, Repsol, BHP, ExxonMobil, US Department of Energy and Sandia National Laboratories), the Department of Energy Center for Subsurface Energy Security, and the Welch Foundation (F-1319).

Appendix A. Supplementary data

Supplementary material related to this article can be found, in the online version, at doi:https://doi.org/10.1016/j.colsurfa.2019.124276.

References

[1] J.L. Dickson, B.P. Binks, K.P. Johnston, Stabilization of carbon dioxide-in-Water emulsions with silica nanoparticles, Langmuir 20 (2004) 7976–7983, https://doi.org/10.1021/la0488102.

[2] M.J. Kadhum, D.P. Swatske, J.H. Harwell, B. Shiau, D.E. Resasco, Propagation of interfacially active carbon nanohybrids in porous media, Energy Fuels 27 (2013) 6518–6527, https://doi.org/10.1021/ef401387j.

[3] R. Ponnapati, O. Karazincir, E. Dao, R. Ng, K.K. Mohanty, R. Krishnamoorti, Polymer-functionalized nanoparticles for improving waterflood sweep efficiency: characterization and transport properties, Ind. Eng. Chem. Res. 50 (2011) 13030–13036, https://doi.org/10.1021/ie2019257.

[4] L.C. Villamizar, P. Lohateeraparp, J.H. Harwell, D.E. Resasco, B.J. Shiau, Dispersion stability and transport of nanohybrids through porous media, Transp Porous Med 96 (2013) 63–81, https://doi.org/10.1007/s11242-012-0073-2.

[5] A.J. Worthen, H.G. Bagaria, Y. Chen, S.L. Bryant, C. Huh, K.P. Johnston, Nanoparticle-stabilized carbon dioxide-in-water foams with fine texture, J. Colloid Interface Sci. 391 (2013) 142–151, https://doi.org/10.1016/j.jcis.2012.09.043.

[6] H.G. Bagaria, B.M. Neilson, A.J. Worthen, Z. Xue, K.Y. Yoon, V. Cheng, et al., Adsorption of iron oxide nanoclusters stabilized with sulfonated copolymers on silica in concentrated NaCl and CaCl2 brine, J. Colloid Interface Sci. 398 (2013) 217–226, https://doi.org/10.1016/j.jcis.2013.01.056.

[7] H.G. Bagaria, Z. Xue, B.M. Neilson, A.J. Worthen, K.Y. Yoon, S. Nayak, et al., Iron oxide nanoparticles grafted with sulfonated copolymers are stable in concentrated brine at elevated temperatures and weakly adsorb on silica, ACS Appl. Mater. Interfaces 5 (2013) 3329–3339, https://doi.org/10.1021/am4003974.

[8] H.G. Bagaria, K.Y. Yoon, B.M. Neilson, V. Cheng, J.H. Lee, A.J. Worthen, et al., Stabilization of Iron oxide nanoparticles in high sodium and calcium brine at high temperatures with adsorbed sulfonated copolymers, Langmuir 29 (2013) 3195–3206, https://doi.org/10.1021/la304496a.

[9] E.L. Foster, Z. Xue, C.M. Roach, E.S. Larsen, C.W. Bielawski, K.P. Johnston, Iron oxide nanoparticles grafted with sulfonated and zwitterionic polymers: high stability and low adsorption in extreme aqueous environments, ACS Macro Lett. 3 (2014) 867–871, https://doi.org/10.1021/mz5004213.

[10] C. Kotsmar, K.Y. Yoon, H. Yu, S.Y. Ryoo, J. Barth, S. Shao, et al., Stable citrate-coated Iron oxide superparamagnetic nanoclusters at high salinity, Ind. Eng. Chem. Res. 49 (2010) 12435–12443, https://doi.org/10.1021/ie1010965.

[11] S. Ryoo, A.R. Rahmani, K.Y. Yoon, M. Prodanović, C. Kotsmar, T.E. Milner, et al., Theoretical and experimental investigation of the motion of multiphase fluids containing paramagnetic nanoparticles in porous media, J. Pet. Sci. Eng. 81 (2012) 129–144, https://doi.org/10.1016/j.petrol.2011.11.008.

[12] Z. Xue, E. Foster, Y. Wang, S. Nayak, V. Cheng, V.W. Ngo, et al., Effect of grafted copolymer composition on Iron oxide nanoparticle stability and transport in porous media at high salinity, Energy Fuels 28 (2014) 3655–3665, https://doi.org/10.1021/ef500340h.

[13] F. Javadpour, J.-P. Nicot, Enhanced CO2 storage and sequestration in deep saline aquifers by nanoparticles: commingled disposal of depleted uranium and CO2, Transp. Porous Media 89 (2011) 265–284, https://doi.org/10.1007/s11242-011-9768-z.

[14] N.K. Maurya, P. Kushwaha, A. Mandal, Studies on interfacial and rheological properties of water soluble polymer grafted nanoparticle for application in enhanced oil recovery, J. Taiwan Inst. Chem. Eng. 70 (2017) 319–330, https://doi.org/10.1016/j.jtice.2016.10.021.

[15] L.M. Corredor, M.M. Husein, B.B. Maini, Impact of PAM-Grafted nanoparticles on the performance of hydrolyzed polyacrylamide solutions for heavy oil recovery at different salinities, Ind. Eng. Chem. Res. 58 (2019) 9888–9899, https://doi.org/10.1021/acs.iecr.9b01290.

[16] A.U. Rognmo, H. Horjen, M.A. Fernø, Nanotechnology for improved CO 2 utilization in CCS: laboratory study of CO 2 -foam flow and silica nanoparticle retention in porous media, Int. J. Greenh. Gas Control. 64 (2017) 113–118, https://doi.org/10.1016/j.ijggc.2017.07.010.

[17] S. Alzobaidi, C. Da, V. Tran, M. Prodanović, K.P. Johnston, High temperature ultralow water content carbon dioxide-in-water foam stabilized with viscoelastic zwitterionic surfactants, J. Colloid Interface Sci. 488 (2017) 79–91, https://doi.org/10.1016/j.jcis.2016.10.054.

[18] Z.A. AlYousef, M.A. Almobarky, D.S. Schechter, The effect of nanoparticle aggregation on surfactant foam stability, J. Colloid Interface Sci. 511 (2018) 365–373, https://doi.org/10.1016/j.jcis.2017.09.051.

[19] Z. AlYousef, M. Almobarky, D. Schechter, Enhancing the stability of foam by the use of nanoparticles, Energy Fuels 31 (2017) 10620–10627, https://doi.org/10.1021/acs.energyfuels.7b01697.

[20] C. Zhang, Z. Li, Q. Sun, P. Wang, S. Wang, W. Liu, CO2 foam properties and the stabilizing mechanism of sodium bis(2-ethylhexyl)sulfosuccinate and hydrophobic nanoparticle mixtures, Soft Matter 12 (2016) 946–956, https://doi.org/10.1039/C5SM01408E.

[21] Z. Xue, A.J. Worthen, C. Da, A. Qajar, I.R. Ketchum, S. Alzobaidi, et al., Ultradry carbon dioxide-in-Water foams with viscoelastic aqueous phases, Langmuir 32 (2016) 28–37, https://doi.org/10.1021/acs.langmuir.5b03036.

[22] J. Lee, E. Moesari, C.B. Dandamudi, G. Beniah, B. Chang, M. Iqbal, et al., Behavior of spherical poly(2-acrylamido-2-methylpropanesulfonate) polyelectrolyte brushes on silica nanoparticles up to extreme salinity with weak divalent cation binding at ambient and high temperature, Macromolecules 50 (2017) 7699–7711, https://doi.org/10.1021/acs.macromol.7b01243.

[23] S. Alzobaidi, M. Lotfollahi, I. Kim, K.P. Johnston, D.A. DiCarlo, Carbon dioxide-in-Brine foams at high temperatures and extreme salinities stabilized with silica nanoparticles, Energy Fuels 31 (2017) 10680–10690, https://doi.org/10.1021/acs.energyfuels.7b01814.

[24] Z. Xue, A. Worthen, A. Qajar, I. Robert, S.L. Bryant, C. Huh, et al., Viscosity and stability of ultra-high internal phase CO2-in-water foams stabilized with surfactants and nanoparticles with or without polyelectrolytes, J. Colloid Interface Sci. 461 (2016) 383–395, https://doi.org/10.1016/j.jcis.2015.08.031.

[25] J.M. Berlin, J. Yu, W. Lu, E.E. Walsh, L. Zhang, P. Zhang, et al., Engineered nanoparticles for hydrocarbon detection in oil-field rocks, Energy Environ. Sci. 4 (2011) 505–509, https://doi.org/10.1039/C0EE00237B.

[26] N. Saleh, H.-J. Kim, T. Phenrat, K. Matyjaszewski, R.D. Tilton, G.V. Lowry, Ionic strength and composition affect the mobility of surface-modified Fe0 nanoparticles in water-saturated sand columns, Environ. Sci. Technol. 42 (2008) 3349–3355, https://doi.org/10.1021/es071936b.

[27] A.J. Worthen, V. Tran, K.A. Cornell, T.M. Truskett, K.P. Johnston, Steric stabilization of nanoparticles with grafted low molecular weight ligands in highly concentrated brines including divalent ions, Soft Matter 12 (2016) 2025–2039, https://doi.org/10.1039/C5SM02787J.
[28] D.H. Napper, Polymeric Stabilization of Colloidal Dispersions, Academic Press Incorporated, 1983.
[29] Y. Wang, H. Zhu, M.D. Becker, J. Englehart, L.M. Abriola, V.L. Colvin, et al., Effect of surface coating composition on quantum dot mobility in porous media, J. Nanopart. Res. 15 (2013) 1805, https://doi.org/10.1007/s11051-013-1805-0.
[30] J.K. Newman, C.L. McCormick, Water-soluble copolymers. 52. Sodium-23 NMR studies of ion-binding to anionic polyelectrolytes: poly(sodium 2-acrylamido-2-methylpropanesulfonate), poly(sodium 3-acrylamido-3-methylbutanoate), poly(sodium acrylate), and poly(sodium galacturonate), Macromolecules 27 (1994) 5114–5122, https://doi.org/10.1021/ma00096a039.
[31] C.G. Sinn, R. Dimova, M. Antonietti, Isothermal titration calorimetry of the Polyelectrolyte/Water interaction and binding of Ca2+: effects determining the quality of polymeric scale inhibitors, Macromolecules 37 (2004) 3444–3450, https://doi.org/10.1021/ma030550s.
[32] Y. Park, C. Huh, J. Ok, H. Cho, One-step synthesis and functionalization of high-salinity-Tolerant magnetite nanoparticles with sulfonated phenolic resin, Langmuir 35 (2019) 8769–8775, https://doi.org/10.1021/acs.langmuir.9b00752.
[33] H.L. Hsieh, A. Moradi-Araghi, G.A. Stahl, I.J. Westerman, Water-soluble polymers for hostile environment enhanced oil recovery applications, Makromol. Chemie Macromol. Symp. 64 (1992) 121–135, https://doi.org/10.1002/masy.19920640113.
[34] C.L. McCormick, D.L. Elliott, Water-soluble copolymers. 14. Potentiometric and turbidimetric studies of water-soluble copolymers of acrylamide: comparison of carboxylated and sulfonated copolymers, Macromolecules 19 (1986) 542–547, https://doi.org/10.1021/ma00157a007.
[35] A.A. Kmetz, M.D. Becker, B.A. Lyon, E. Foster, Z. Xue, K.P. Johnston, et al., Improved mobility of magnetite nanoparticles at high salinity with polymers and surfactants, Energy Fuels 30 (2016) 1915–1926, https://doi.org/10.1021/acs.energyfuels.5b01785.
[36] C.A. Zuniga, J.B. Goods, J.R. Cox, T.M. Swager, Long-term high-temperature stability of functionalized graphene oxide nanoplatelets in Arab-D and API brine, ACS Appl. Mater. Interfaces 8 (2016) 1780–1785, https://doi.org/10.1021/acsami.5b09656.
[37] P. Auroy, L. Auvray, L. Léger, Silica particles stabilized by long grafted polymer chains: from electrostatic to steric repulsion, J. Colloid Interface Sci. 150 (1992) 187–194, https://doi.org/10.1016/0021-9797(92)90279-U.
[38] P. Akcora, H. Liu, S.K. Kumar, J. Moll, Y. Li, B.C. Benicewicz, et al., Anisotropic self-assembly of spherical polymer-grafted nanoparticles, Nat. Mater. 8 (2009) 354–359, https://doi.org/10.1038/nmat2404.
[39] K. Ueno, A. Inaba, M. Kondoh, M. Watanabe, Colloidal stability of bare and polymer-grafted silica nanoparticles in ionic liquids, Langmuir 24 (2008) 5253–5259, https://doi.org/10.1021/la704066v.
[40] Y.-P. Wang, X.-W. Pei, X.-Y. He, K. Yuan, Synthesis of well-defined, polymer-grafted silica nanoparticles via reverse ATRP, Eur. Polym. J. 41 (2005) 1326–1332, https://doi.org/10.1016/j.eurpolymj.2004.12.010.
[41] C. Li, B.C. Benicewicz, Synthesis of well-defined polymer brushes grafted onto silica nanoparticles via surface reversible addition−Fragmentation chain transfer polymerization, Macromolecules 38 (2005) 5929–5936, https://doi.org/10.1021/ma050216r.
[42] E.E. Ureña-Benavides, E.L. Lin, E.L. Foster, Z. Xue, M.R. Ortiz, Y. Fei, et al., Low adsorption of magnetite nanoparticles with uniform polyelectrolyte coatings in concentrated brine on model silica and sandstone, Ind. Eng. Chem. Res. 55 (2016) 1522–1532, https://doi.org/10.1021/acs.iecr.5b03279.
[43] M. Iqbal, B.A. Lyon, E.E. Ureña-Benavides, E. Moaseri, Y. Fei, C. McFadden, et al., High temperature stability and low adsorption of sub-100 nm magnetite nanoparticles grafted with sulfonated copolymers on Berea sandstone in high salinity brine, Colloids Surf. A Physicochem. Eng. Asp. 520 (2017) 257–267, https://doi.org/10.1016/j.colsurfa.2017.01.080.
[44] S. Kralj, M. Drofenik, D. Makovec, Controlled surface functionalization of silica-coated magnetic nanoparticles with terminal amino and carboxyl groups, J. Nanopart. Res. 13 (2011) 2829–2841, https://doi.org/10.1007/s11051-010-0171-4.
[45] Dhs are given in nm with cumulative % volume in parenthesis. n.d.
[46] H.C. Allen, D.E. Gragson, G.L. Richmond, Molecular structure and adsorption of dimethyl sulfoxide at the surface of aqueous solutions, J. Phys. Chem. B 103 (1999) 660–666, https://doi.org/10.1021/jp9820323.
[47] L. Novák, I. Bányai, J.É Fleischer-Radu, J. Borbély, Direct amidation of poly (γ-glutamic acid) with benzylamine in dimethyl sulfoxide, Biomacromolecules 8 (2007) 1624–1632.
[48] I.M. Kolthoff, M.K. Chantooni, S. Bhowmik, Dissociation constants of uncharged and monovalent cation acids in dimethyl sulfoxide, J. Am. Chem. Soc. 90 (1968) 23–28, https://doi.org/10.1021/ja01003a005.
[49] F.G. Bordwell, Algrim Donald. Nitrogen acids. 1. Carboxamides and sulfonamides, J. Org. Chem. 41 (1976) 2507–2508, https://doi.org/10.1021/jo00876a042.
[50] C. McCallum, A.D. Pethybridge, Conductance of acids in dimethyl-sulphoxide—II. Conductance of some strong acids in DMSO at 25°C, Electrochim. Acta 20 (1975) 815–818, https://doi.org/10.1016/0013-4686(75)87002-2.
[51] M.R. Crampton, I.A. Robotham, Acidities of some substituted ammonium ions in DimethylSulfoxide†, J. Chem. Res. (S) (1997) 22–23, https://doi.org/10.1039/A606020J.
[52] R.M. Lanigan, T.D. Sheppard, Recent developments in amide synthesis: direct amidation of carboxylic acids and transamidation reactions, Eur. J. Org. Chem. 2013 (2013) 7453–7465, https://doi.org/10.1002/ejoc.201300573.
[53] S. Čampelj, D. Makovec, M. Drofenik, Functionalization of magnetic nanoparticles with 3-aminopropyl silane, J. Magn. Magn. Mater. 321 (2009) 1346–1350, https://doi.org/10.1016/j.jmmm.2009.02.036.
[54] G. Fritz, V. Schädler, N. Willenbacher, N.J. Wagner, Electrosteric stabilization of colloidal dispersions, Langmuir 18 (2002) 6381–6390, https://doi.org/10.1021/la015734j.
[55] M. Ranka, P. Brown, T.A. Hatton, Responsive stabilization of nanoparticles for extreme salinity and high-temperature reservoir applications, ACS Appl. Mater. Interfaces 7 (2015) 19651–19658, https://doi.org/10.1021/acsami.5b04200.